Double-negative T resident memory cells of the lung react to influenza virus infection via CD11c^{hi} dendritic cells

K Neyt[1,2], CH GeurtsvanKessel[3] and BN Lambrecht[1,2,4]

Immunity to Influenza A virus (IAV) is controlled by conventional TCRαβ$^+$ CD4$^+$ and CD8$^+$ T lymphocytes, which mediate protection or cause immunopathology. Here, we addressed the kinetics, differentiation, and antigen specificity of CD4$^-$CD8$^-$ double-negative (DN) T cells. DNT cells expressed intermediate levels of TCR/CD3 and could be further divided in γδ T cells, CD1d-reactive type I NKT cells, NK1.1$^+$ NKT-like cells, and NK1.1$^-$ DNT cells. NK1.1$^-$ DNT cells had a separate antigen-specific repertoire in the steady-state lung, and expanded rapidly in response to IAV infection, irrespectively of the severity of infection. Up to 10% of DNT cells reacted to viral nucleoprotein. Reinfection experiments with heterosubtypic IAV revealed that viral replication was a major trigger for recruitment. Unlike conventional T cells, the NK1.1$^-$ DNT cells were in a preactivated state, expressing memory markers CD44, CD11a, CD103, and the cytotoxic effector molecule FasL. DNT cells resided in the lung parenchyma, protected from intravascular labeling with CD45 antibody. The recruitment and maintenance of CCR2$^+$ CCR5$^+$ CXCR3$^+$ NK1.1$^-$ DNT cells depended on CD11c^{hi} dendritic cells (DCs). Functionally, DNT cells controlled the lung DC subset balance, suggesting they might act as immunoregulatory cells. In conclusion, we identify activation of resident memory NK1.1$^-$ DNT cells as an integral component of the mucosal immune response to IAV infection.

INTRODUCTION

Mucosal tissues such as the lung are frequently exposed to pathogens that can cause life-threatening pulmonary infections. These infectious agents like influenza A virus (IAV) must be quickly and efficiently controlled by the immune system, without causing overt damage to the gas exchange apparatus of the lung.[1] Upon IAV infection, CD103$^+$ and CD11b$^+$ dendritic cells (DCs) take up and process viral particles and migrate to the mediastinal lymph node where they encounter naïve CD4$^+$ and CD8$^+$ T cells.[2] These T cells undergo a stepwise process of activation, proliferation, and differentiation toward a helper or cytotoxic phenotype, respectively, and migrate back to the lung as effector cells in a process requiring the chemokine receptors CCR2, CCR5, and CXCR3.[3,4] CD8 effector T cells are crucial for viral clearance, but their effector functions need tight regulation since they can also cause immunopathology and damage to the lung microenvironment.[5,6] CD4 T cells promote CD8 T-cell and B-cell responses to IAV infection, although they are not critical for this process.[7–10] Adoptive transfer studies demonstrated that CD4 T cells are also able to control viral load and exert direct cytotoxic effector functions in the lung environment,[11,12] yet the contribution of CD4 T-cell cytotoxicity to viral clearance *in vivo* in the lungs is modest.[13]

As acute infections are cleared, effector CD8 T cells further differentiate into KLRG-1^{hi} CD127^{lo} short-lived effector cells and CD127^{hi} memory precursor effector cells capable of generating long-lived memory CD8 T cells, and a similar process occurs in CD4 T cells.[14,15] Long-lived memory cells can recirculate via lymphoid organs as T central memory cells (T_{cm}), patrol in and out peripheral tissues as T effector memory (T_{em}) cells or reside for prolonged periods in the lungs as T resident memory cells (T_{rm}), which express high levels of CD69, CD11a, and/or CD103.[15] Triggered by retained antigen

[1]VIB Inflammation Research Center, Laboratory of Immunoregulation, Ghent, Belgium. [2]Department of Respiratory Medicine, Ghent University, Ghent, Belgium. [3]Department of Viroscience, Erasmus MC, Rotterdam, The Netherlands and [4]Department of Pulmonary Medicine, Erasmus MC, Rotterdam, The Netherlands. Correspondence: BN Lambrecht (bart.lambrecht@ugent.be)

Received 1 March 2015; accepted 22 July 2015; published online 16 September 2015. doi:10.1038/mi.2015.91

presented by DCs, CD4 T_{rm} and CD8 T_{rm} cells were shown to reside for months in the lungs of IAV-infected mice and -infected volunteers, thus providing immunity against reinfection with the same or heterologous strain of influenza.[15–22]

Non-conventional T cells that express a functional T cell receptor (TCR) but lack expression of CD4 and CD8 co-receptors (therefore called double-negative (DN) T cells) can be observed in various disease models in human and mice, in which they were attributed different functions.[23] The lungs are one of the many tissues where DNT cells were described in steady state and following insults to the lung.[24–30] As DNT cells are defined by exclusion, they are very heterogeneous, arising either from the thymus or extrathymically. Classical DNT cells express intermediate levels of αβTCR, and are different from type I CD1d-restricted invariant natural killer T cells and γδTCR$^+$ T cells that are often found to lack CD4 and CD8 expression, and therefore fall under the DNT definition.[31,32]

The involvement of the different DNT cells in IAV infection is currently unknown. We therefore carefully addressed the phenotype, origin, antigen specificity and TCR repertoire, kinetics of recruitment and activation, and acquisition of effector and memory markers of αβTCR$^+$ DNT cells, and conventional T cells during and following infection with the H3N2 X31 IAV strain or reinfection with the heterosubtypic H1N1 PR8 IAV strain. We observed a predominant accumulation of NK1.1$^-$ αβTCR$^+$ DNT cells in the lung after primary influenza infection, but not after heterosubtypic infection and these cells had characteristics of T_{rm} cells situated in the lung interstitium. The induction and maintenance of the NK1.1$^-$ DNT cell response was dependent on lung DCs that caused DNT accumulation through recruitment. Functionally these cells may act as immunoregulatory cells by controlling the lung DC subset balance.

RESULTS

Influenza infection induces accumulation of unconventional CD4$^-$CD8$^-$ DNT cells in the lung

Studies on T-cell responses to airway infection with IAV (H3N2, strain X31) have mainly focused on major histocompatibility complex (MHC)-I-restricted CD8$^+$ and MHCII-restricted CD4$^+$ conventional T cells, which can be easily identified within the αβTCR$^+$ CD3$^+$ cell population of a lymphocyte gate (FSC^{lo} SSC^{lo}) on dispersed lung cells (**Figure 1a**, population A and B respectively). Within these αβTCR$^+$ lymphocytes, a CD4$^-$CD8$^-$ DN population can be consistently observed. As this population of DNT cells is defined mainly by exclusion of CD4 and CD8 expression, we sought to further define it using multi-color flowcytometry.[26] A significant proportion of CD3$^+$ DNT cells expressed a γδTCR receptor (**Figure 1a**, population C), consistent with the notion that pulmonary γδ T cells often lack expression of CD4 and CD8. Another well-known population of unconventional T cells are NKT cells, sharing some phenotypic markers with NK cells (NK1.1 expression in C57Bl/6 mice), variably expressing CD4 depending on tissue residence, and many of which can be identified by staining with α-galactosylceramide-loaded CD1d tetramers (TMs). Based on CD1d TM binding and NK1.1 expression, lung DNT cells could be further classified as DN type I NKT cells (**Figure 1a**, population D). After gating out γδ T cells and type I NKT cells, the remaining lung DNT cells could be further divided into NK1.1$^-$ CD1d TM$^-$ αβTCR$^+$ DNT cells (**Figure 1a**, population E) and NK1.1$^+$ CD1d TM$^-$ αβTCR$^+$ DNT cells (**Figure 1a**, population F). Whether NK1.1 expression represents an activation state of some lymphocytes or a truly different cell population of DN NKT-like cells remains a matter of debate.[33,34] Up to 15% of NK1.1$^-$ CD1d TM$^-$ αβTCR$^+$ DNT expressed B220, a marker previously found on peripheral DNT cells (data not shown). All DNT cells including the NK1.1$^-$ CD1d TM$^-$ αβTCR$^+$ DNT cells expressed intermediate TCR levels compared with conventional CD4 or CD8 T cells, a finding previously also reported for other DNT cells (**Figure 1a**, histograms).[24]

We next analyzed the relative distribution and kinetics of accumulation of all DNT subsets following IAV or mock infection. Both in mock- and IAV-infected mice, CD4$^+$ and CD8$^+$ conventional T cells represented the majority of T cells in the lung 9 days post infection (d.p.i.), unconventional T cells each representing less than 2.5% of T cells (**Figure 1b**). When absolute numbers of DNT cells were studied over time (**Figure 1c**), only the population of NK1.1$^-$ CD1d TM$^-$ αβTCR$^+$ DNT cells expanded significantly following infection, in a kinetic that closely resembled the expansion of CD4 and CD8 conventional T cells (**Figure 1e**). The more than 20-fold expansion of NK1.1$^-$ αβTCR$^+$ DNT cells at the peak of the response (8 d.p.i.) was followed by a steep contraction phase also seen in conventional T cells. As the NK1.1$^-$ CD1d TM$^-$ αβTCR$^+$ population is the only one that is induced after infection, this is the population that was studied in further detail and will be called NK1.1$^-$ DNT cells throughout the paper.

Figure 1 αβ TCR^{int} double-negative T (DNT) cells accumulate in the lungs of influenza virus-infected mice. (**a**) Gating strategy used to subdivide the T-cell populations into conventional CD4$^+$ (population A) and CD8$^+$ (population B) T cells and non-conventional T cells: γδ TCR$^+$ DNT cells (population C), αβ TCR$^+$ CD1d TM$^+$ DNT cells (type I NKT, population D), αβ TCR$^+$ CD1d TM$^-$ NK1.1$^-$ DNT cells (population E), and αβ TCR$^+$ CD1d TM$^-$ NK1.1$^+$ DNT cells (population F). As an example, plots were generated 9 d.p.i. Histograms show αβ TCR expression intensity on lymphocyte subsets: CD4$^+$ T cells (black), CD8$^+$ T cells (black dashed line), and the total CD4$^-$CD8$^-$ T cells population (red) on the upper panel, type I NKT (black dashed line), NK1.1$^-$ DNT cells (gray filled line), and NK1.1$^+$ DNT cells (black). (**b**) Distribution of conventional and non-conventional T-lymphocyte subsets in the lungs 9 d.p.i. after X31 (black) or mock (white) virus infection, expressed as % of total CD3$^+$ alive T cells. (**c**) Kinetics of accumulation of non-conventional T cells in the lungs of X31 (black) or mock (white) virus-infected mice. (**d**) Kinetics of accumulation of conventional CD4$^+$ (squares) and CD8$^+$ (dots) T cells in the lungs of X31 (black) or mock (white) virus-infected mice. (**e**) CD4 and CD8 expression profiles of αβ TCR$^+$ T cells (left) and γδ TCR$^+$ T cells (right) in the lungs of athymic nude mice (lower row) compared with one wild-type mouse (WT; upper row) at 2 d.p.i. and absolute cell number of conventional and non-conventional T cells. Cells were pregated as singlets, alive, CD19$^-$, and CD3$^+$. All experiments were performed at least twice and figures are representative for each separate experiment.

Origin of lung DNT cells

We next addressed the origin of the DNT cells of the lungs, which can develop like classical T cells in the thymus or outside of the thymus. DNT cells of the gut have indeed been described in thymectomized mice, but the origin of lung DNT cells is less clear.[35–37] We therefore infected athymic nude-Foxn1^{nu} mice and defined T-cell subsets 2 d.p.i. Some remaining αβ and γδ T cells could be observed, and there was a shift toward more

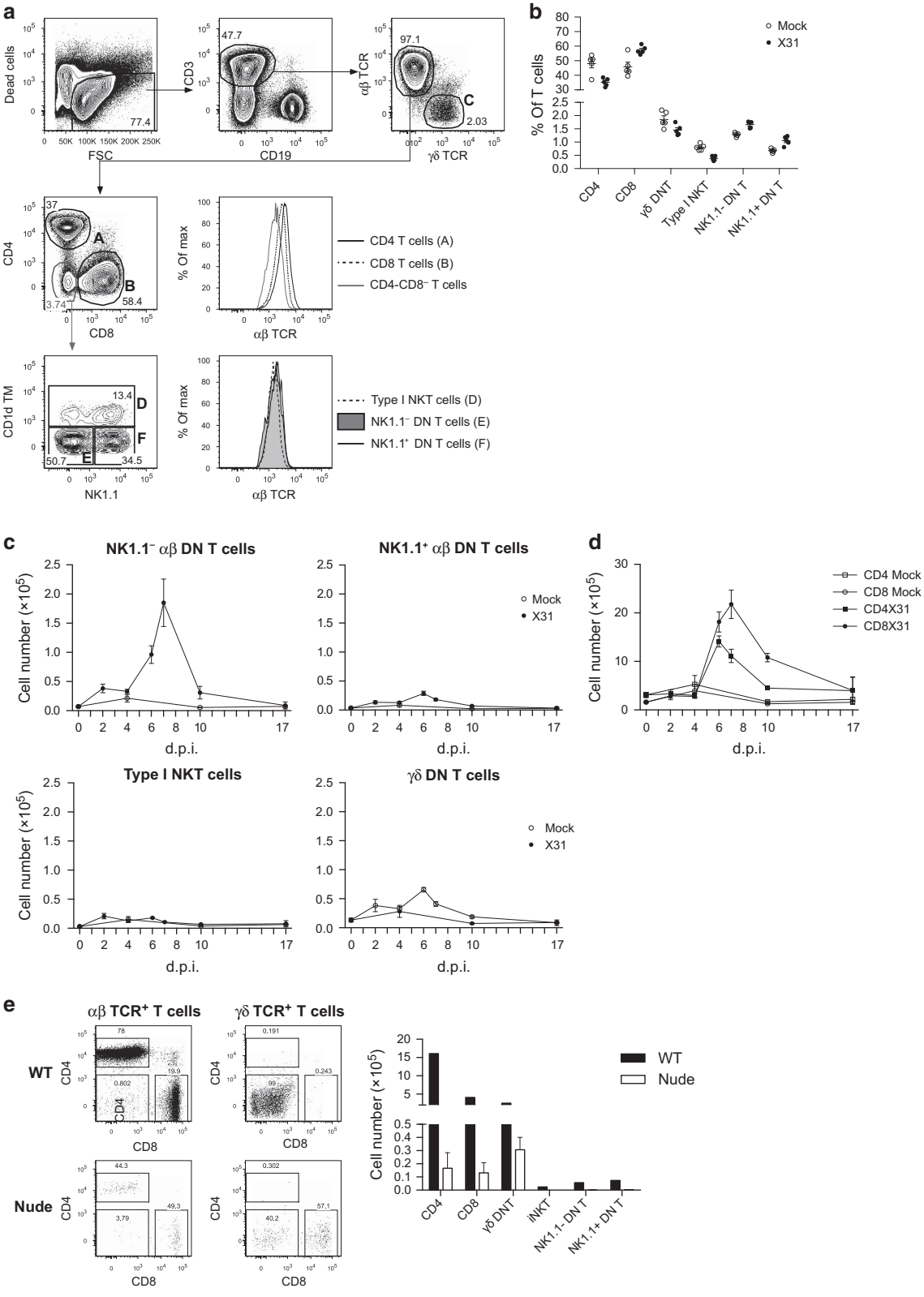

$CD8^+$ γδ T cells in athymic nude-Foxn1^{nu} mice, consistent with the notion that many γδ T cells develop extrathymically. Some lung $CD4^+$ and $CD8^+$ αβTCR$^+$ T cells were still present, indicative of extrathymic development (**Figure 1d**). Unexpectedly, lung DNT cells were almost completely lacking in Foxn1^{nu} mice. These observations point toward a thymic origin of the type I NKT, NK1.1$^-$, and NK1.1$^+$ DNT cell populations during IAV infection.

NK1.1$^-$ DNT cells resemble CD8 T cells

As DNT cells are defined by lack of CD4 and CD8, and as the kinetics of accumulation, and the thymic origin closely resembled those of conventional T cells, we questioned whether some of the DNT cells represent revertant conventional T cells, losing surface expression of CD4 and/or CD8 after ligation of the TCR, as previously described.[38] NK1.1$^-$ DNT cells and conventional T cells were therefore sorted from lungs 9 d.p.i. T-cell lineage determination is molecularly controlled by the balance between Thpok (promoting CD4 T cell differentiation) and Runx3 (promoting CD8 T cell differentiation) transcription factors.[39] Like $CD8^+$ conventional T cells, NK1.1$^-$ DNT cells had low expression of the CD4 lineage transcription factor Thpok by quantitative PCR and were negative for the transcription factor Rorγt that is typical for Th17 and some subsets of γδT cells (data not shown). Expression of the CD8 lineage transcription factor Runx3 was lower in NK1.1$^-$ DNT cells than in conventional $CD8^+$ T cells but higher than in $CD4^+$ T cells. Although the ratio of Runx3 over Thpok suggests that NK1.1$^-$ DNT cells are transcriptionally more related to $CD8^+$ T cells than to $CD4^+$ T cells (**Figure 2a**), these results do not show a clear bias toward CD4 or CD8 lineage imprinting for the entire NK1.1$^-$ DNT cell population. Intracellular staining for CD8 and CD4 revealed that 10% of the NK1.1$^-$ DNT cells had intracytoplasmic CD8 (but not CD4) expression (**Supplementary Figure S1** online) to the same extent as conventional CD8 T cells, indicating that at least part of the DNT cells might indeed be revertant CD8 T cells.

TCR repertoire of NK1.1$^-$ DNT cells

Following influenza infection, conventional CD8 T cells react to a restricted set of immunodominant epitopes derived from various antigens, and these CD8 T cells undergo oligoclonal expansion. Indeed, at 8 d.p.i., close to 40% of the lung conventional $CD8^+$ T cells had a receptor specific for the IAV nucleoprotein (NP) peptide ASNENMETM, as revealed by TM staining using the K^b-ASNENMETM TM (**Figure 2b**). A considerable proportion of NK1.1$^-$ DNT cells also stained for this TM, but at the peak of the response, this fraction represented only 10% of DNT cells followed by a slow contraction phase (**Figure 2b**).

To further delineate if there would be oligoclonal expansion of DNT cells resembling the one seen in CD8 T cells, we performed a more elaborate profiling of TCR Vβ usage at T-cell population level in subsets of lung T cells (**Figure 2c**). In mock-infected animals, Vβ usage was broad across conventional CD4 and CD8 T cells, whereas in NK1.1$^-$ DNT cells, there was an overrepresentation of Vβ 8.1/8.2 cells to 14% of the repertoire. As previously reported, the entire influenza-specific CD8 T-cell pool has a TCR Vβ repertoire skewed toward TCR Vβ8.3, Vβ4, and Vβ7[40] and type I NKT express an oligoclonal TCR repertoire (Vα 14)[41,42] combined with one of three Vβ chains (Vβ2, Vβ7, Vβ8.2). Whereas in CD8 T cells there was enrichment for Vβ7 and Vβ8.3 in the total pool of CD8 T cells following influenza infection, there was no further enrichment in NK1.1$^-$ DNT cells post infection and TCR Vβ8.1/8.2 and 5.1/5.2 remained the most prominently expressed TCR Vβ in the total NK1.1$^-$ DNT population. In $NP_{ASNENMETM}$-reactive CD8 T cells, there was strong enrichment for Vβ4 and Vβ8.3 usage, and the same phenomenon was seen in $NP_{ASNENMETM}$-reactive NK1.1$^-$ DNT cells.

Effector functions of NK1.1$^-$ DNT cells

As at least some NK1.1$^-$ DNT cells were transcriptionally related to CD8 T cells and shared NP-reactivity with CD8 T cells, we measured some of the effector molecules involved in CD8 function. An increase in Granzyme B content of $CD4^+$, $CD8^+$, and NK1.1$^-$ DNT cells was observed in reaction to IAV infection already 4 d.p.i., compared with mock-infected mice. The difference in mean fluorescence intensity between mock- and virus-infected mice was 441, 648, and 773 for $CD4^+$, $CD8^+$, and NK1.1$^-$ DNT cells, respectively (**Figure 2d**). At 9 d.p.i., however, the Granzyme B content was further increased in all cell types. Conventional $CD8^+$ T cells showed the largest increase in Granzyme B content with a difference in mean fluorescence intensity of 5018 compared with mock-infected mice, whereas the difference in mean fluorescence intensity for $CD4^+$ T cells and NK1.1$^-$ DNT cells was 1,631 and 2,242, respectively (**Figure 2d**). Perforin expression did not change dramatically upon virus infection compared with mock-infected mice (**Figure 2d**).

Conventional CD8 T-cell–mediated cell killing is not only induced via release of intracellular Granzyme B, but it can also be mediated via surface expression of FasL (CD95L). In mock-infected animals, NK1.1$^-$ DNT cells expressed the highest level of FasL, followed by $CD8^+$ conventional T cells that expressed significantly more FasL than $CD4^+$ T cells. After IAV infection, FasL was upregulated further, but only in CD4 T cells this reached statistical significance (**Figure 2e**).

Conventional cytotoxic T cells are a major source of interferon (IFN)-γ during infection. The IFN-γ production was indeed increased in $CD8^+$ T cells after IAV infection. In NK1.1$^-$ DNT cells, however, the capacity to produce IFN-γ was reduced upon IAV infection (**Figure 2f**). This suppression of cytokine production might indicate that the NK1.1$^-$ DNT cells have an exhausted phenotype after IAV infection. One of the signs of T-cell exhaustion is expression of the co-inhibitory B7 family receptor PD-1 on the cell surface. Upon IAV infection, PD-1 was expressed on about 60% of CD4 T cells and 70% of CD8 T cells. In contrast, the percentage of PD-1 expression on NK1.1$^-$ DNT cells was low (20%) and did not increase upon infection (**Figure 2g**). Therefore, NK1.1$^-$ DNT cells are unlikely to become exhausted upon IAV infection.

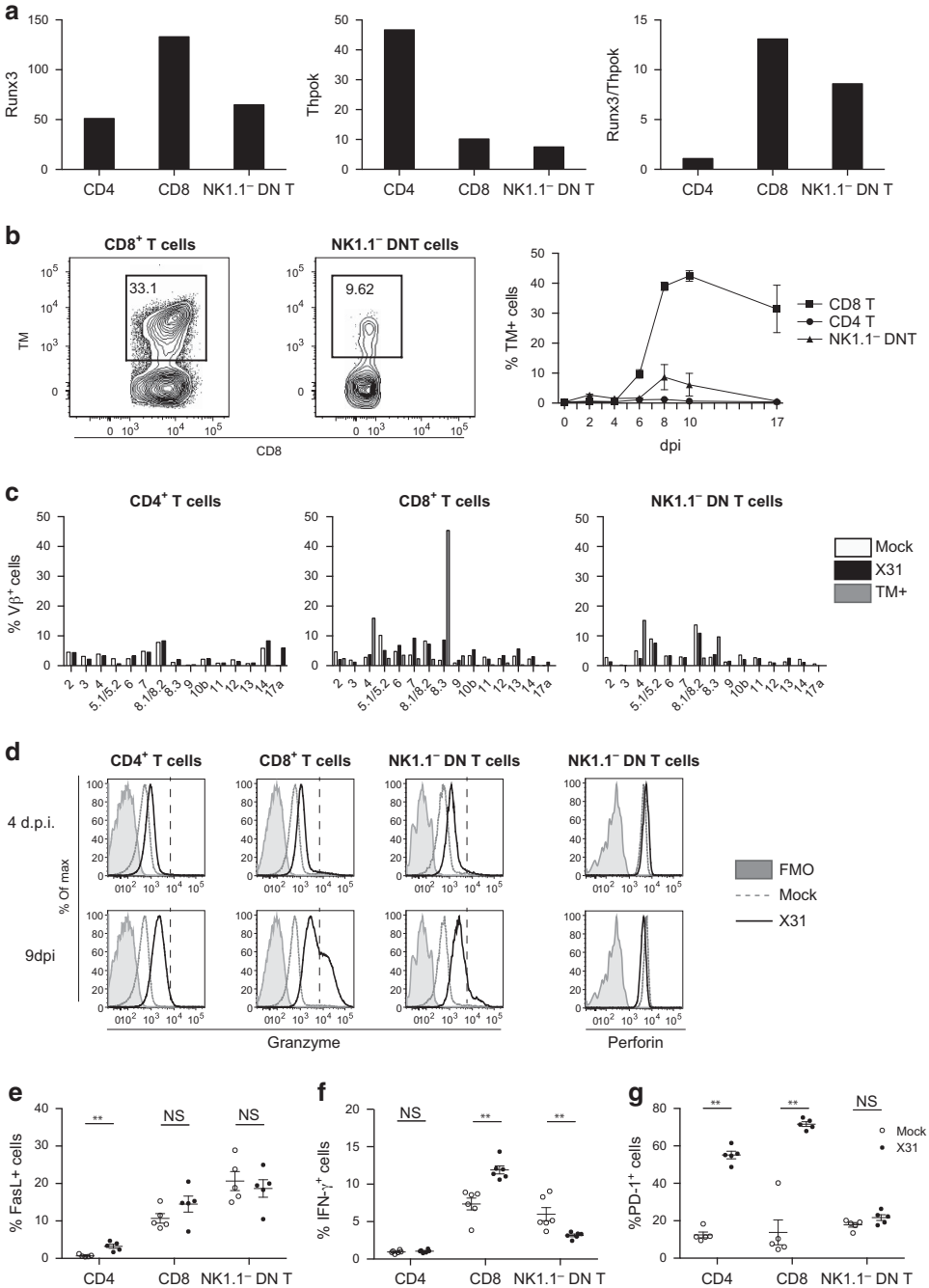

Figure 2 NK1.1$^-$ DNT cells are transcriptionally related to CD8 T cells, yet have a different T-cell repertoire. (**a**) Quantification of the expression level of *Runx3* (CD8 lineage) and *Thpok* (CD4 lineage) by quantitative PCR on sorted CD4, CD8, and NK1.1$^-$ DNT cells from the lungs of X31 virus-infected mice 8 d.p.i. Expression levels were normalized to expression of the housekeeping gene *hprt*. (**b**) NP tetramer staining (K^b-ASNENMETM) of CD8 and NK1.1$^-$ DNT cells on lungs of X31-infected mice 8 d.p.i. and kinetic of TM$^+$ T cells expressed as percentage of CD4 (dots), CD8 (squares), or αβ TCR$^+$ CD1d TM$^-$ NK1.1$^-$ DNT cells (triangles). (**c**) Screening of the T-cell receptor Vβ repertoire of CD4, CD8, and NK1.1$^-$ DNT cells in the pooled lungs of 6 mock-infected (white bars) and 6 X31-infected (black bars, TM$^+$ cells: gray bars) mice 8 d.p.i. expressed as % of CD4, CD8, or NK1.1$^-$ DNT cells. (**d**) Quantification of granzyme B (left) and perforin (right) expression on CD4, CD8, and NK1.1$^-$ DNT cells in the lungs of X31- (black line) or mock-infected (gray line) mice 4 d.p.i. (upper panel) and 9 d.p.i. (lower panel). The FMO staining for granzyme and perforin is indicated as a filled gray line. (**e**) Quantification of FasL expression on CD4, CD8, and NK1.1$^-$ DNT cells in the lungs of X31- (black) or mock-infected (white) mice 9 d.p.i. (**f**) Quantification of IFN-γ production by CD4, CD8, and NK1.1$^-$ DNT cells in the lungs of X31- (black) or mock-infected (white) mice. Lung cells were isolated 9 d.p.i. and restimulated for 4 h with $NP_{ASNENMETM}$ peptide in the presence of Golgi Stop before staining for IFN-γ. (**g**) Expression of exhaustion marker PD-1 was determined on CD4 and CD8 T cells and NK1.1$^-$ DNT cells 9 days after mock (white) or X31 (black) infection. All experiments were performed at least two times and figures are representative for every separate experiment. $^{**}P<0.01$, $^{*}P<0.05$. NS = not statistically significant different.

Lung NK1.1$^-$ DNT cells display an activated phenotype of resident memory T cells

The high levels of surface FasL and intermediate levels of intracellular IFN-γ present already in mock-infected mice suggested that lung NK1.1$^-$ DNT cells might be in a pre-activated state before infection. To address this issue further, we employed a panel of T-cell activation markers. In mock-infected animals, up to 20% of lung conventional T cells expressed the memory/effector T-cell marker CD44, whereas close to 80% of NK1.1$^-$ DNT cells expressed CD44 (**Figure 3a**). At 4 d.p.i., CD44 expression was further induced on CD8 T cells, and by 9 d.p.i., when the virus was cleared, 60–80% of conventional T cells expressed CD44 (**Figure 3b**). Expression of CD44 on NK1.1$^-$ DNT cells remained high at 9 d.p.i. The early activation marker CD69 was induced on all studied T cells after IAV infection; 25% of NK1.1$^-$ DNT cells expressed CD69, whereas only 15% of CD4 T cells and 5% of CD8 T cells expressed CD69 at 4 d.p.i. (**Figure 3c**). Even at 9 d.p.i., the levels of CD69 were still elevated on all subsets (**Figure 3d**).

During the clearance of respiratory virus infection, conventional effector T cells can give rise to different cell fates, either giving rise to immediate and short-lived effector cells or giving rise to effector cells with the potential to generate long-lived memory cells.[43] The phenotype and fate of CD44^{hi} effector T cells can be studied in more detail by using the markers KLRG1 and CD127 (ref. 14; **Figure 3e**). Within the CD8$^+$CD44$^+$ effector memory population (population A), short-lived effector cells are enriched in the KLRG1$^+$CD127$^-$ cells (population D), whereas memory precursor effector cells are enriched in the KLRG1$^-$CD127$^+$ population of cells (population E; **Figure 3e**). Whereas this staining has mainly been employed to follow the fate of CD8$^+$ T cells, we also employed it to CD4$^+$ and NK1.1$^-$ DNT cells (**Figure 3e**). In mock-infected cells, very few NK1.1$^-$ DNT cells expressed KLRG1 indicative of immediate effector potential, whereas a major population of CD127$^+$ memory cells was observed. Viral infection mainly led to expansion of KLRG1$^-$CD127$^-$ early effector cells (population C; **Figure 3e**), of which the ultimate fate is hard to predict.

Memory cells can reside in the central lymphoid organs (as T central memory cells, T_{cm}) and recirculate via the blood to other lymphoid tissues. Alternatively, a considerable part of antiviral memory T cells reside in peripheral tissues as T resident memory (T_{rm}) cells.[44] T_{rm} cells have been identified by expression of various markers including CD69, CD103, and CD11a.[15,44] In the lung, T_{rm} cells are hard to discriminate from recirculating blood T_{cm} or naïve T cells that firmly adhere to lung capillaries, even after extensive flushing of the lung capillary bed. To delineate intravascular DNT cells and conventional T cells simultaneously, we injected an AF700-labeled antibody to the pan leukocyte marker CD45 intravenously, and obtained blood and lung homogenates 5 min after injection. Using this labeling protocol, 100% of circulating peripheral blood CD3$^+$ T cells was readily labeled with AF700-CD45 (**Figure 4a**). In mock-infected cells (**Figure 4b**), the majority of lung CD4 and CD8 T cells were labeled with CD45, demonstrating that most lung lymphocytes were still in the lung vascular pool, even after extensive exsanguination and flushing. The majority of lung NK1.1$^-$ DNT cells were protected from CD45 *in vivo* labeling already in mock-infected mice (**Figure 4b**), identifying these cells as tissue resident cells. At 9 d.p.i., up to 90% of lung conventional CD4 and CD8 T cells were protected from CD45 labeling and these cells also expressed CD69 (data not shown), as previously described.[3,15] Tissue resident lymphocytes express various levels of CD11a and/or CD103.[3,15] Like CD4 and CD8 T_{rm} cells, 10–15% of CD45$^-$ NK1.1$^-$ DNT cells co-expressed CD11a and CD103 and around 60–70% expressed CD11a but not CD103 (**Figure 4c**).

Reinfection with homologous or heterologous virus does not trigger NK1.1$^-$ DNT accumulation

Primary infection with IAV led to induction of an immune response of antigen-specific conventional T cells and NK1.1$^-$ DNT cells, which acquired T_{em} and T_{rm} memory characteristics, and conventional T cells have been shown to control heterosubtypic immunity to re-exposure with a heterologous virus.[45] We therefore set up primary infections using X31 (H3N2) followed by reinfection with the same X31 or the PR8 (H1N1) virus to test the reactivity of DNT cells to reinfection with the same or heterologous virus. X31 usually causes a mild and self-limiting viral infection, whereas PR8 leads to progressive infection that ultimately leads to death. We therefore used a much lower inoculum of PR8 virus to reinfect (5 $TCID_{50}$ compared with 1×10^5 $TCID_{50}$ for the X31 virus). In the mice that first received a mock infection, comparisons between X31 and PR8 primary infection were possible. Owing to the low inoculum, PR8 infection initially led to less weight loss compared with the higher inoculum of X31, but nevertheless caused more weight loss when infection advanced to 8 d.p.i. The amount of NK1.1$^-$ DNT cells obtained after infection with the X31 virus at 8 d.p.i. was not significantly different from the amount obtained after infection with the PR8 (H1N1) virus, despite the observed difference in weight loss at 8 d.p.i. (**Figures 5a and b**, mock-X31 versus mock-PR8). As expected, when mice were first infected with X31, re-infection with X31 did not cause weight loss, as replication and infection was prevented due to antibody-mediated sterilizing immunity. There was, however, an increased accumulation of CD8$^+$ and CD4$^+$ conventional T cells, whereas NK1.1$^-$ DNT cells failed to expand (X31-X31 versus X31-mock). Boosting of cellular immunity was most likely due to enhanced presentation of opsonized viral antigens, as antibodies to H3 and N2 are induced in these mice. Upon reinfection with the heterologous PR8 virus, heterosubtypic CD8 T cell–mediated immunity has been described to protect mice from becoming sick[46] and consequently mice did not loose weight (X31-PR8 versus mock-PR8). In these mice, there was no boosting of conventional CD4$^+$, CD8$^+$, or NK1.1$^-$ DNT cells. When we studied NP-specific T cells, re-infection of mice led to strong increases in NP-specific CD8$^+$ conventional T cells in mice reinfected

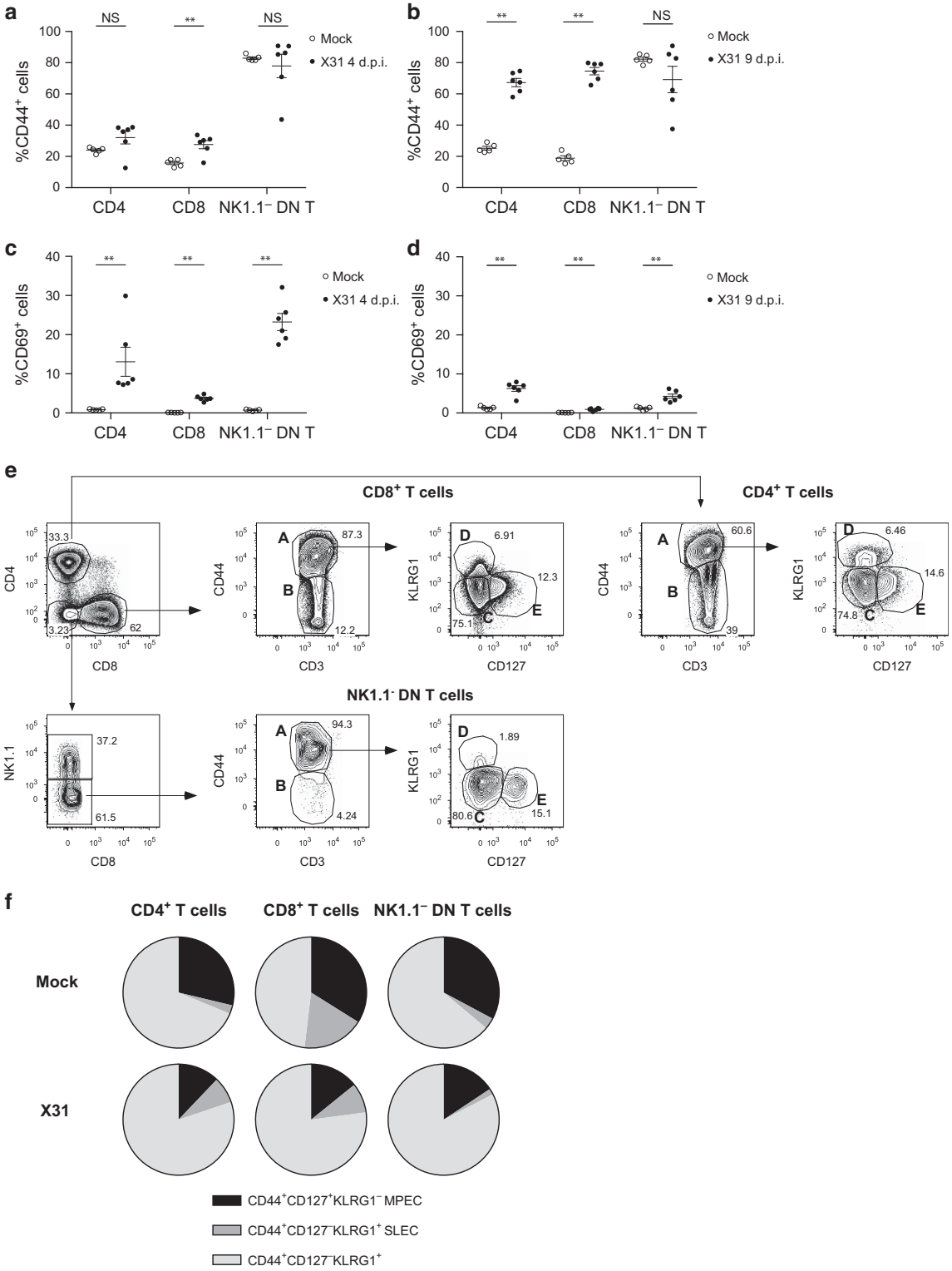

Figure 3 NK1.1$^-$ double-negative T (DNT) cells display a pre-activated memory phenotype and expand as KLRG1$^-$ CD127$^-$ cells. (**a**) Mice were infected with X31 (black) or mock (white) virus, at 4 d.p.i., the expression of the memory marker CD44 was measured in conventional and NK1.1$^-$ DNT cells, gated as in **Figure1**. (**b**) Identical analysis at 9 d.p.i. (**c**) Identical analysis for CD69 at 4 d.p.i. (**d**) Identical analysis for CD69 at 9 d.p.i. (**e**) Gating strategy for studying the phenotype of memory T cells. T cells were gated as CD3$^+$ CD19$^-$ αβ TCR$^+$ cells. Memory T cells were gated as CD44$^+$ (population A), naïve cells were gated as CD44$^-$ (population B). On memory cells, KLRG1$^-$CD127$^-$ cells were effector cells (population C, T_{eff}), KLRG1$^+$CD127$^-$ cells were identified as short-lived effector memory cells (population D, SLEC), and KLRG1$^-$CD127$^+$ cells are memory precursor effector cells (population E, MPEC). (**f**) Distribution of the memory populations (MPEC: black, SLEC: dark gray and KLRG1$^-$CD127$^-$ cells: light gray) of CD4, CD8, and NK1.1$^-$ DNT cells the lungs of X31- or mock-infected mice 9 d.p.i. expressed as percentage of CD44$^+$ cells. All experiments were performed at least twice and figures are representative for every separate experiment. $^{**}P<0.01$, $^{*}P<0.05$. NS = not statistically significant different.

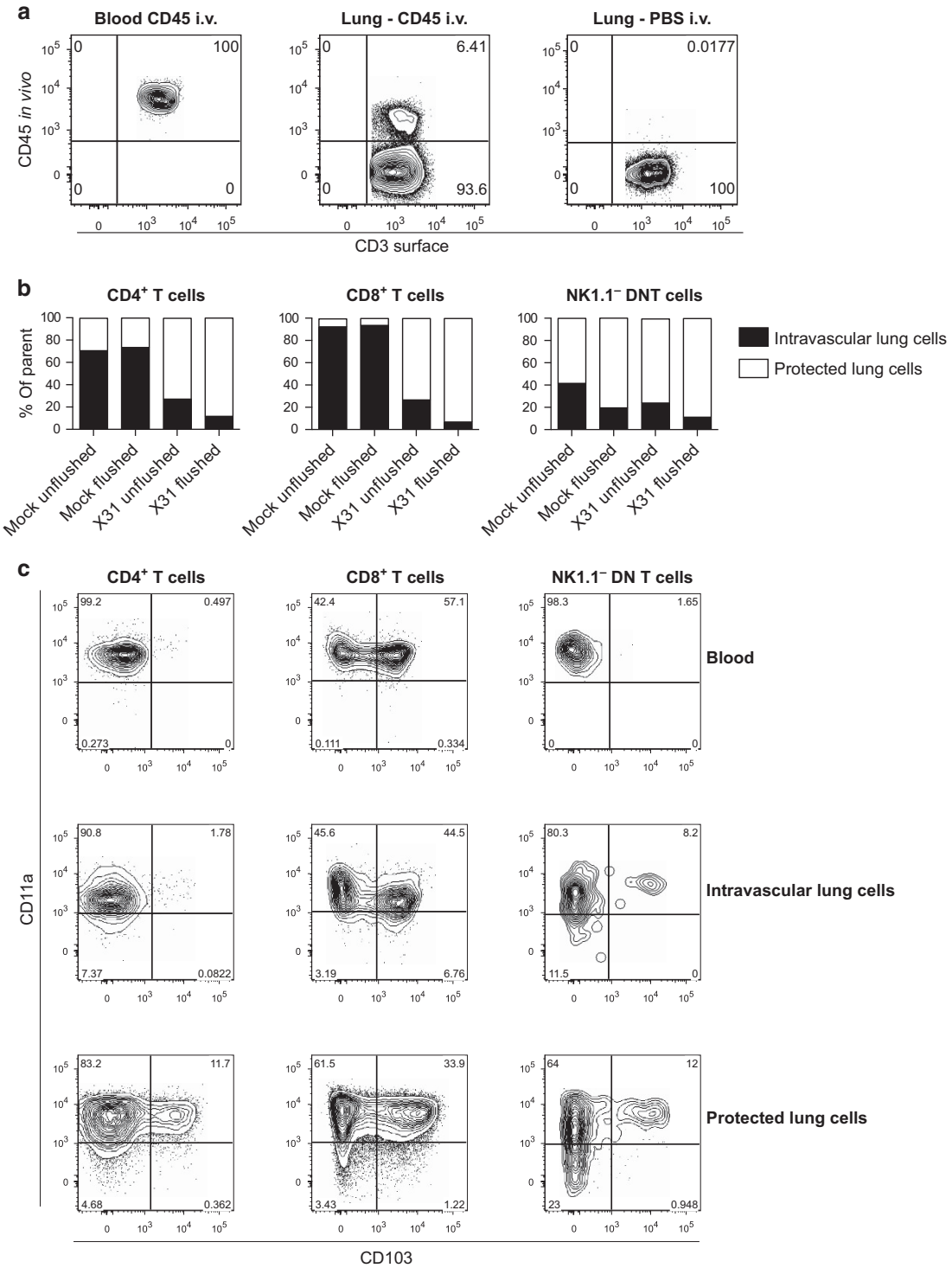

Figure 4 NK1.1$^-$ double-negative T (DNT) cells are protected from intravenous CD45 staining and have a T_{rm} phenotype. (**a**) *In vivo* labeling of circulatory T cells by intravenous injection of an AF700-labeled antibody against CD45 or PBS 6 d.p.i. combined with an *in vitro* staining of surface CD3 on blood and lung cells. Gated on living CD3$^+$ αβ TCR$^+$ cells. (**b**) Proportion of protected CD45$^-$ cells (white boxes) and intravascular CD45$^+$ cells (black boxes) within conventional CD4$^+$ or CD8$^+$ T cells and NK1.1$^-$ DNT cells. (**c**) CD11a and CD103 expression on CD45$^+$ blood cells (upper panel), intravascular CD45$^+$ lung cells (middle panel), and protected CD45$^-$ lung cells (lower panel). Cells were gated as in **Figure 1**, but images were acquired from mechanically dispersed lung cells, after performing bronchoalveolar lavage. All experiments were performed twice and figures are representative for every separate experiment.

with X31 and PR8, but no such increase was seen in NK1.1$^-$ DNT cells (**Figure 5c**). Together, these observations suggested that viral replication and/or a strong inflammatory signal is needed to induce NK1.1$^-$ DNT cells. In contrast to conventional CD8 T cells, NK1.1$^-$ DNT cells did not mount a recall response upon the mere presentation of viral antigens.

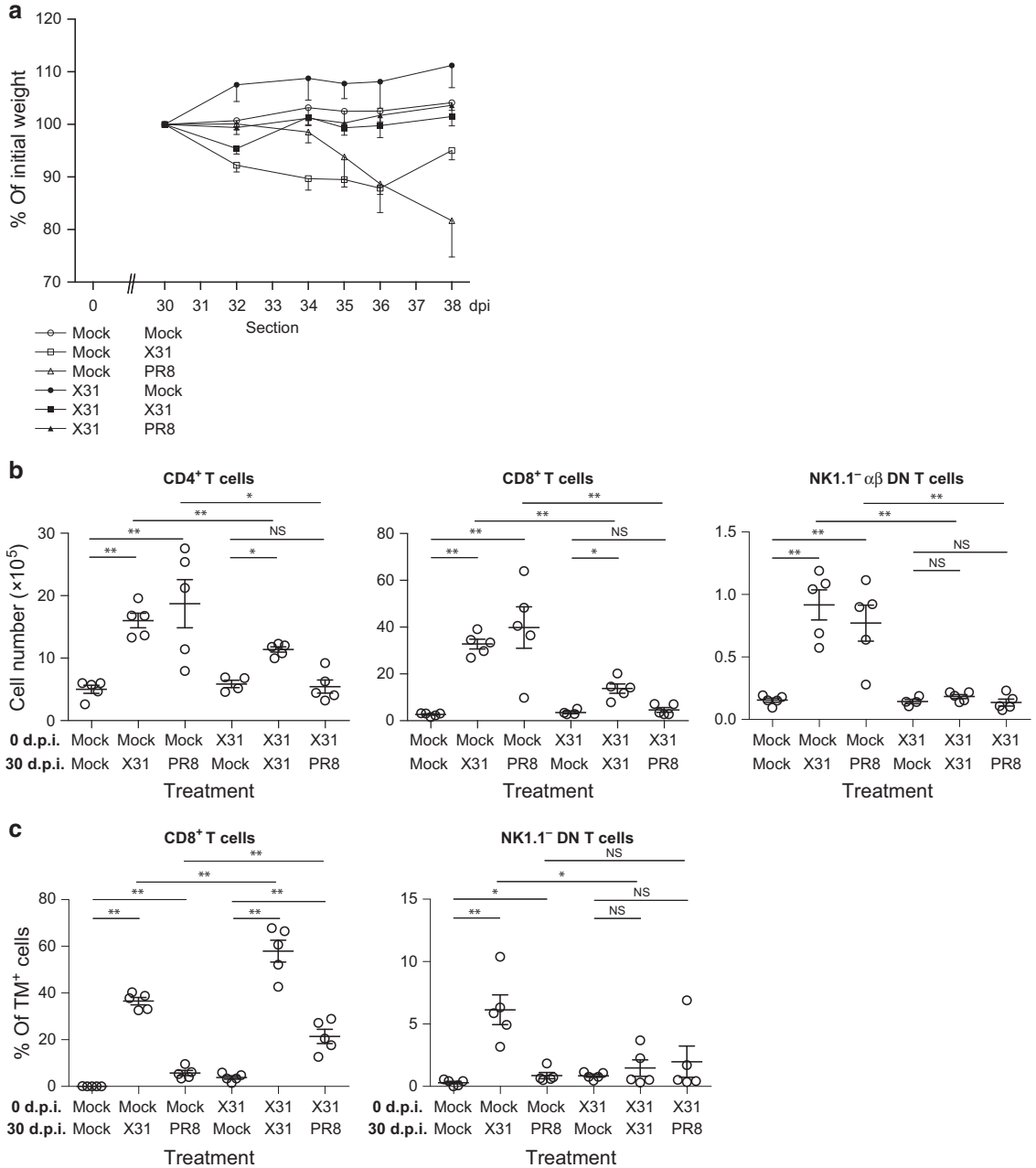

Figure 5 Viral replication triggers accumulation of NK1.1$^-$ double-negative T (DNT) cells irrespective of severity of infection. (**a**) Weight loss after second infection expressed as % of initial weight: Mock (dots), X31 (squares), and PR8 (triangles) after mock (white) or X31 (black) infection. (**b**) Quantification of conventional and NK1.1$^-$ DNT cells after primo infection or reinfection with the same or with a heterologous virus, carrying shared nucleoprotein T-cell antigens, yet lacking overlapping hemagglutinin and neuraminidase to which neutralizing antibodies are generated. Mice were first infected with mock or X31 (H3N2) virus and reinfected with mock, X31 (H3N2), or PR8 (H1N1) virus 30 d.p.i. Lungs were analyzed 38 days after initial infection. (**c**) Proportion of TM$^+$ conventional CD8$^+$ T cells and NK1.1$^-$ DNT cells 38 d.p.i. All experiments were performed at least two times and figures are representative for every separate experiment. $^{**}P<0.01$, $^{*}P<0.05$. NS = not statistically significant different.

Induction and maintenance of the NK1.1$^-$ DNT response depends on chemokine production by conventional DCs

The increased numbers of NK1.1$^-$ DNT cells in the lungs of primary infected, but not reinfected, mice could be due to increased local proliferation or local recruitment of T cells with T_{em} or T_{rm} phenotype. To address this, we injected 5-bromo-2'-deoxyuridine (BrdU) and measured instantaneous cell division by measuring BrdU uptake in conventional and DNT cells 3.5 h later. Whereas 14% and 24% of conventional CD4 and CD8 T cells, respectively, were dividing within the 3.5 h pulse-chase experiment at 6 d.p.i., only a minority of NK1.1$^-$ DNT cells incorporated BrdU (**Figure 6a**), indicating that local proliferation is unliklely to be the explanation for the increase in NK1.1$^-$ DNT cell numbers. We next

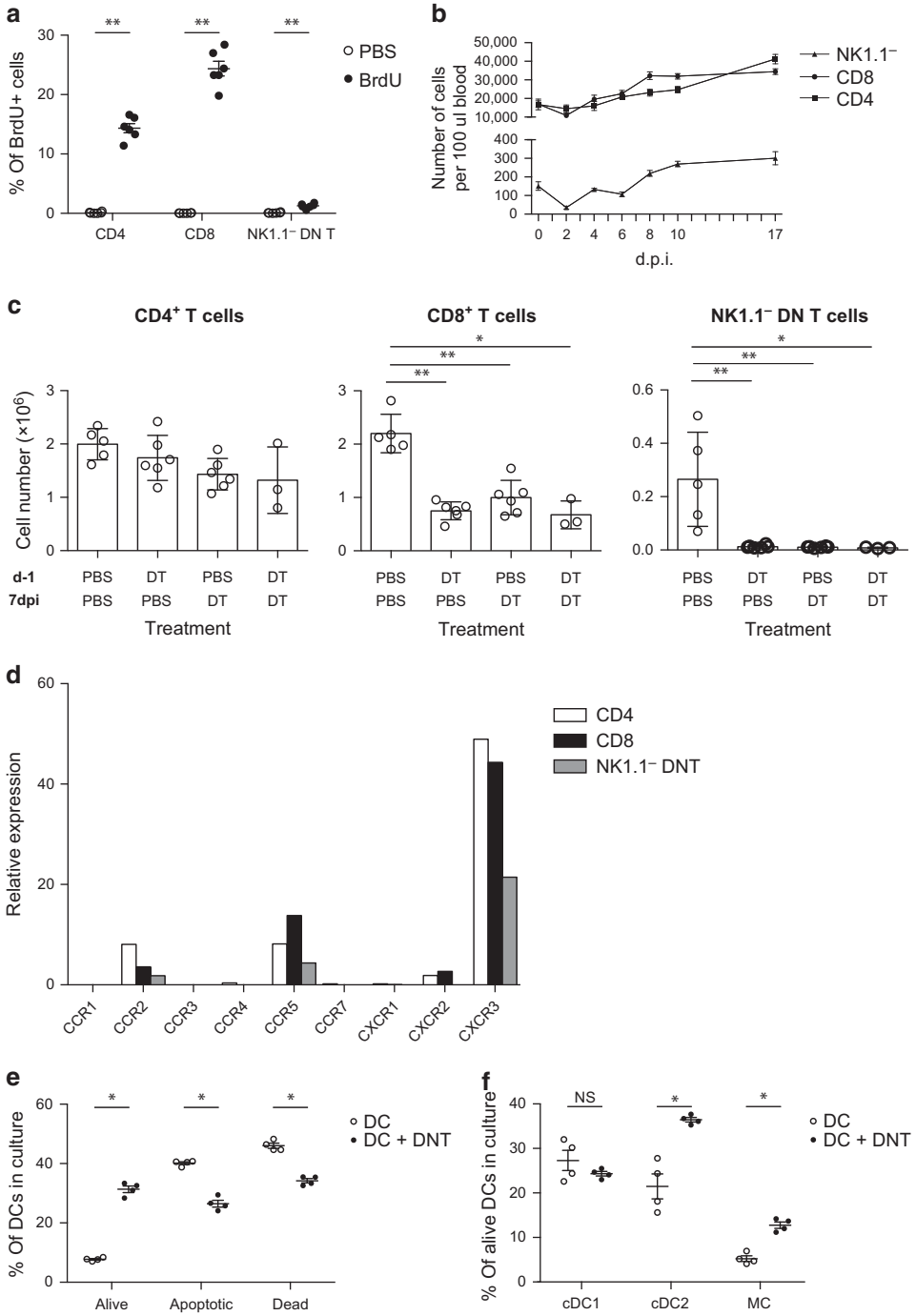

Figure 6 NK1.1$^-$ double-negative T (DNT) cells are recruited from the blood in a DC-dependent manner and control the DC subset balance. (**a**) 5-Bromo-2'-deoxyuridine (BrdU) expression on conventional CD4 and CD8 T cells and NK1.1$^-$ DNT cells 3.5 h after i.v. injection of BrdU (black) or PBS (white). (**b**) Kinetics of conventional CD4 (squares) and CD8 (circles) T cells and NK1.1$^-$ DNT cells (triangles) per 100 µl blood after X31 infection. (**c**) CD11c DTR chimeric mice were injected with PBS or DT 1 day before infection with X31 virus or 7 d.p.i. CD4, CD8, and NK1.1$^-$ DNT cells in the lungs were quantified 9 d.p.i. (**d**) Quantitative PCR analysis of the chemokine receptor repertoire of sorted CD4 (white bars), CD8 (black bars), and NK1.1$^-$ DNT (gray bars) cells from the lungs of mice infected with X31 8 d.p.i.; expression levels were normalized for expression of the housekeeping gene *hprt*. (**e**) Proportion of alive, apoptotic (Annexin V$^+$), and dead (7AAD$^+$) pulmonary DCs in culture after 36 h of co-culture with (black) or without (white) sorted DNT cells. (**f**) Proportion of the alive pulmonary DC subsets in culture after 36 h of co-culture with (black) or without (white) DNT cells. All experiments were performed two times and figures are representative for every separate experiment. $^{**}P<0.01$, $^{*}P<0.05$. NS = not statistically significant different.

infected mice and measured the amount of NK1.1$^-$ DNT cells per 100 µl of whole blood every other day following infection. A drop early after infection followed by an increase suggested that increased recruitment from the bloodstream is causing the increase in pulmonary NK1.1$^-$ DNT cells (**Figure 6b**) after infection.

Previously, we and others have found that CD11c^{hi} airway DCs are crucial for the recruitment, restimulation, and retention of conventional CD4 and CD8 T_{em} cells to the lungs, by acting as professional antigen presenting cells for effector T cells, and by producing chemokines and cytokines involved in T-cell recruitment and homeostasis.[2,47–50] To investigate whether NK1.1$^-$ DNT cells are similarly dependent on CD11c^{hi} DCs, CD11c DTR chimeric mice that carry the diphtheria toxin (DT) receptor behind the CD11c promotor only in hematopoietic cells were infected with X31 IAV. As previously reported, administration of DT efficiently depleted all hematopoietic CD11c$^+$ cells from the lungs (**Supplementary Figure S2**).[48] DT was administered either 1 day before infection, 7 d.p.i., or at both time points and numbers of conventional CD4$^+$ and CD8$^+$ T cells, as well as NK1.1$^-$ DNT cells were analyzed 2 days after the last treatment (9 d.p.i.). As shown in **Figure 6c**, the accumulation of cytotoxic CD8$^+$ T cells was strongly reduced in infected DT-treated mice, when treatment was given before or after primary infection. Likewise, the accumulation of NK1.1$^-$ DNT cells was strongly reduced in animals given DT early and late in infection. However, CD4$^+$ T cells were not reduced by DT treatment early in infection, and only minor reductions of CD4$^+$ T cells were seen when DT was given late in infection.

Lung CD8 T cells are recruited by DCs to the lung interstitium via production of CCL3, CCL4, CCL5, and CXCL10, acting on chemokine receptors CCR2, CCR5, and CXCR3. To investigate which DC-derived chemokines could signal to NK1.1$^-$ DNT cells to attract or maintain them in the lung, CD4$^+$, CD8$^+$, and NK1.1$^-$ DNT cells were sorted from the lung 8 d.p.i. Like conventional CD8 T cells, NK1.1$^-$ DNT cells expressed CCR2, CCR5, and CXCR3, suggesting that DCs might induce recruitment and retention of these cells via these chemokine receptor interactions (**Figure 6d**).

NK1.1$^-$ DNT cells balance the ratio of DC subsets

We finally wanted to address the potential function of NK1.1$^-$ DNT cells recruited to the lungs by CD11c^{hi} cells. In transplantation and autoimmunity models, it has been suggested that DNT cells have an immunoregulatory capacity by controlling DCs,[51] and the fact that CD11c^{hi} cells attracted these cells, led us to study the impact of NK1.1$^-$ DNT cells on DCs. We therefore performed an experiment in which we sorted lung DCs (carefully excluding CD11c^{hi} macrophages) and NK1.1$^-$ DNT cells from the lungs of infected mice at 9 d.p.i. and co-cultured them for 36 h. We observed that the presence of DNT cells stimulated the survival of lung DCs in culture, whereas in the absence of sorted DNT more apoptotic and dead cells were present in the culture (**Figure 6e**). CD11c^{hi} cells of the lungs can be divided in CD103$^+$ cDC_1, CD11b$^+$ cDC_2, and CD64$^+$ monocyte-derived cells. Within the total population of CD11c^{hi} lung cells, only CD11b$^+$ DCs and monocyte-derived cells had a survival benefit.

DISCUSSION

Before the discovery of NKT cells, CD4$^-$CD8$^-$ DNT cells were found as a major fraction of lung lymphocytes, expressing an intermediate level of TCR, and representing up to 20–60% of all lung CD3$^+$ cells.[52] However, as NKT cell and γδ TCR-specific antibodies have been used in combination with the α-galactosylceramide CD1d TM in multi-color flowcytometry, the frequency of classical TCR^{int} DNT cells was found to be much lower, in the range of 1–2% of lung CD3$^+$ T lymphocytes.[28,32] We found that the only population of DNT cells that accumulated following IAV infection with X31 or PR8 infection was characterized by intermediate expression of αβTCR, yet lacking expression of NK1.1. Analysis of α-galactosylceramide CD1d TMs showed that these cells were not type I NKT cells. A minor contamination of NKT-like cells or type II NKT cells in the CD1d TM$^-$ NK1.1$^-$ DNT cell gate cannot be excluded as those cells can also lose expression of NK1.1.[53,54]

The precise origin of these cells has been unclear, but it has been suggested that they originate from the thymus by escaping negative selection.[55,56] The fact that the numbers of TCR^{int} DNT cells are unaffected in the lungs of athymic nude mice, led to the suggestion that these cells might also arise extrathymically, very similar to the intraepithelial lymphocytes of the lamina propria of the gut.[27,28] However, in our hands, the number of DNT cells in the lungs was severely reduced in athymic mice. This suggests that NK1.1$^-$ DNT cells develop via the thymus. In the context of immune activation, some T cells might downregulate TCR expression after cognate ligand–MHC recognition and downregulate CD8 membrane expression, which could also lead to a very similar phenotype of TCR^{int} DNT cells.[38] Intracytoplasmic staining for CD4 and CD8 did, however, not reveal evidence for selective down-regulation of membrane CD4 expression and only a small fraction of NK1.1$^-$ DNT cells showed intracellular CD8 expression. The Vβ repertoire of the NK1.1$^-$ NKT cells was distinct from the Vβ repertoire of CD4 and CD8 T cells. Furthermore, the Vβ repertoire was not skewed toward a NKT[57,58] or MAIT cell[58,59] usage. However, staining with a K^b-NP TM did reveal some MHCI-restricted antigen specificity shared with conventional CD8 cytotoxic T cells. Lineage-specific transcription factor analysis also demonstrated that a part of the NK1.1$^-$ DNT cells were more related to CD8 than to CD4 T cells. Together, these data suggest that some 10% of NK1.1$^-$ DNT cells represent antigen-specific CD8 T cells that have lost surface expression of CD8, while maintaining it in the cytoplasm. Studies in human systemic lupus erythematosus patients have shown that DNT cells can originate from CD8 T cells by upregulation of the CREMα transcription factor that in turn represses expression of the *CD8A* and *CD8B* gene.[60,61] As we found residual cytoplasmic expression of CD8 in 10% of DNT cells, this is an unlikely scenario.

One clear difference between lung CD8$^+$ and NK1.1$^-$ DNT cells was the steady-state activation state in the lung. Indeed, the majority of lung NK1.1$^+$ DNT cells were CD44^{hi}, whereas a majority of CD8$^+$ T cells was CD44^{neg} in the mock-infected lung. Studying lymphocytes in the lung is not straightforward, as the lung is a highly vascularized organ and houses a major reservoir of recirculating naïve or T_{cm} lymphocytes in the lung

capillaries. These lymphocytes cannot always be removed by flushing the lung vasculature with phosphate-buffered saline (PBS) via the pulmonary artery. One way of reliably studying conventional T_{rm} cells is to *in vivo* label these cells by intravenous injection of antibodies to CD4 or to CD8, labeling mainly the intravascular pool of lymphocytes, followed by *ex vivo* staining for other surface markers, labeling all lymphocytes.[3,62] Because of their tissue residence around large airways, T_{rm} cells are protected from labeling by intravenously (i.v.) injected antibody. These studies have been performed using antibodies to CD4 or CD8, but these antibodies were not useful for identifying DNT cells *in vivo*. To delineate intravascular DNT cells and conventional T cells simultaneously, we developed an *in vivo* labeling method employing the pan leukocyte marker CD45, effectively labeling 100% of circulating peripheral blood $CD3^+$ T cells and a majority of lung CD4 and CD8 T lymphocytes, demonstrating that most of the lung conventional lymphocytes in the resting lung are in the lung vascular pool, even after extensive exsanguination and flushing. Only after IAV infection, 90% of lung conventional CD4 and CD8 T cells were protected from *in vivo* CD45 labeling and these cells also variably expressed CD69, CD11a, and CD103, as previously described for T_{rm} cells and thus validating the use of CD45 labeling.[3,15] On the contrary, the majority of lung $NK1.1^-$ DNT cells were already protected from CD45 *in vivo* labeling in the steady-state mock-infected lung, and expressed high levels of CD11a identifying these cells as T_{rm} cells. This is also the reason why the levels of CD44 were so different between $CD8^+$ and $NK1.1^-$ DNT cells, as they were representing the differences between naïve and memory cells, respectively. The activated phenotype was previously also reported in human patients with cutaneous leishmaniasis[63] and tuberculosis.[64] The memory profile of $NK1.1^-$ DNT cells argues against a MAIT cell phenotype or contamination as MAIT cell are reported to have a mostly naïve phenotype in mice[65] and MAIT cell activation is not observed in *in vitro* viral infection models.[66]

Heterosubtypic immunity (HSi) to different strains of IAV that differ in hemaglutinin and neuraminidase is poorly understood but very desirable if we are to develop a universal IAV vaccine. It is generally believed to be mediated by T lymphocytes that reside in the lung as T_{rm} cells, a phenotype also seen in $NK1.1^-$ DNT cells before and following infection. One striking finding in our study, however, was that reinfection with heterosubtypic virus did not lead to expansion of lung $NK1.1^-$ DNT cells, despite the fact that these cells expressed a phenotype of $CD44^{hi}$, $CD11a^{hi}$ T_{rm} cells, and some had specificity for viral NP. A lack of further expansion upon reinfection with heterologous virus does not prove that these cells have no role in mediating HSI. A study using depleting antibodies is, however, very difficult to design as $NK1.1^-$ DNT cells are defined by lack of expression of markers. We initially set up experiments in athymic nude mice so that we could use depleting anti-CD3 antibodies to deplete DNT cells. Unfortunately, however, lung DNT cells were already depleted in athymic mice.

Previous studies on the function of DNT cells in lung immunity have led to conflicting results, possibly due to differences in models used. In a passive transfer model of DNT cells to immunodeficient mice, there was no protection offered against respiratory infection with *Rhodococcus equi*.[67] However, in a model of *Francisella tularensis* respiratory infection, DNT cells were found to be a prominent source of IFN-γ and interleukin-17 early, but not late after infection.[30] In our hands, $NK1.1^-$ DNT cells made IFN-γ but no interleukin-17 after restimulation with $NP_{ASNENMETM}$ peptide (data not shown) and IFN-γ was downregulated by IAV infection. We have purified $NK1.1^-$ DNT cells and adoptively transferred them to other mice in an attempt to study the function of these cells that were recruited to the lungs after IAV infection (data not shown). Unfortunately, the numbers of cells were too low to perform conclusive adoptive transfer studies. We can therefore only speculate on the potential role of $NK1.1^-$ DNT cells in IAV, guided by experiments from the past.

An important consideration is that $NK1.1^-$ DNT cells might have immunoregulatory capacity as they closely resemble the DNT regulatory cells that control allograft rejection by specifically killing Ag-specific effector T cells with the same specificity or by killing DCs in a FasL-dependent manner.[51,68] One striking observation was that 20% of the lung $NK1.1^-$ DNT cells expressed high levels of FasL in steady-state lung. However, when we cultured lung $NK1.1^-$ DNT cells together with lung DCs, we found that the presence of DNT cells did not kill DCs, but rather led to a higher percentage of DCs in the culture, mainly attributable to an increased survival of $CD11b^+$ cDC_2 DCs and monocyte-derived cells, whereas $CD24^+$ cDC_1 DCs were not affected by the presence or absence of DNT cells. Thus, interaction of DNT cells with certain DC subsets turns them less sensitive to apoptosis. As DNT cells were previously described to interact with other cell types such as CD8 and CD4 T cells, B cells, macrophages, and NK cells,[69] it remains an interesting topic to study the interaction of DNT cells with several types of immune cells and to determine whether they can exert different functions depending on the cell type they interact with.

In human studies, DNT cells are often reported to be correlated with progression or severity of disease. DNT cells decrease upon HIV disease progression[70] and are inversely correlated with disease activity in rheumatoid arthritis.[71] In contrast, DNT cells are increased during severe *M. tuberculosis* infection compared with non-severe *M. tuberculosis* infections[64] and during active Sjögren's syndrome,[72] in which the level of DNT cells correlates with the degree of tissue inflammation.[73] Although the fact that DNT cells contract quickly after viral clearance (8 d.p.i.) and thus correlate with the kinetic of disease, we could not confirm a relationship with severity of infection as there was no significant difference between the amounts of DNT cells after X31 or PR8 infection that cause different degrees of weight loss. Future experiments will have to address whether this subset of lung DNT cells has an influence on pulmonary immunity and regulates the severity of immunopathology to variants of IAV.

In conclusion, we have carefully characterized a subset of NK1.1$^-$ DNT cells that resides as a preactivated T_{rm}-like cell in the lung parenchyma, protected from i.v. labeling. This population rapidly expands in response to IAV infection in a process requiring CD11c^{hi} DCs, and has the capacity to balance the ratio of DC subsets. Future studies, in which these cells might be depleted selectively using genetic tools will, have to address whether these cells are beneficial or harmful to the outcome of IAV infection.

METHODS

Mice. C57Bl/6 and athymic nude-Foxn1^{nu} mice (8–10 weeks) were purchased from Harlan Laboratories (Horst, The Netherlands). CD11c-DTR Tg (H2-D^b) mice were bred and housed in specific pathogen-free conditions. All experiments were performed on four to six mice per group, unless mentioned otherwise.

Ethics statement. All experiments were approved by the independent animal ethics committees "Ethische Commissie Dierproeven—faculteit Geneeskunde en Gezondheidswetenschappen Universiteit Gent" (identification number: ECD 13/05) and "Ethische Commissie Proefdieren—faculteit Wetenschappen Universiteit Gent en VIB-site Ardoyen" (identification number: EC 2013_002). Animal care and used protocols adhere to the Belgian Royal Degree of 29 May 2013 for protection of experimental animals. European guideline 2010/63/EU is incorporated in this Belgian legislation.

Influenza virus infection. Mice were infected intranasally with 10^5 $TCID_{50}$ H3N2 X-31 influenza virus, 5 $TCID_{50}$ H1N1 PR8 influenza virus (Medical Research Council, Cambridge, England), or mock (allantoic fluid of uninfected eggs); all diluted in 50 µl PBS.

For reinfection experiments, mice were infected with 10^5 $TCID_{50}$ X-31 or mock virus and were reinfected 30 days later with 3×10^5 $TCID_{50}$ X-31, 5 $TCID_{50}$ PR8, or mock virus diluted in 50 µl PBS. Weight loss was monitored daily.

Isolation of lung cells. Mice were killed and bronchoalveolar lavage was performed by injecting three times 1 ml EDTA-containing PBS through a tracheal catheter before isolating the lungs. For some experiments, lungs were additionally flushed with 20 ml PBS through the right heart ventricle before isolation. Single-cell lung suspensions were prepared by digestion in collagenase/DNase solution for 30 min at 37 °C. After digestion, the suspension was filtered over an 100-µm filter and red blood cells were lysed with osmotic lysis buffer.

Flowcytometry and cell sorting. T-cell staining was done by using CD3 (PE-Cy7 and eFl450, eBioscience, Temse, Belgium; APC, BD Biosciences), CD4 (conjugated to PE-TxR, Invitrogen, Gent, Belgium; PE-Cy5 and FITC, eBioscience, Erembodegem, Belgium), CD8a (conjugated to efluor450 and PE-Cy7, eBioscience; PerCp, BioLegend, London, UK; PE-Cy5, BD Biosciences), CD19 (conjugated to APC, BD Biosciences; AF700 and PE-Cy5, eBioscience), NK1.1 (conjugated to BV605, BioLegend; PE-Cy7, BD Biosciences), CD1d TM (conjugated to PE and APC, NIH TM core facility), αβTCR (conjugated to APC-Cy7, BioLegend), γδTCR (conjugated to FITC, BD Biosciences), NP TM (conjugated to PE, loaded with ASNENMETM peptide, Pelimer, Sanquin), and a fixable live/dead marker in eFl506 (eBioscience). Following additional extracellular markers were used: B220 (conjugated to PE, BD Biosciences; AF700, eBioscience), CD44 (conjugated to AF700, BD Biosciences), CD127 (conjugated to PE-CF594, BD Biosciences), KLRG1 (conjugated to APC, eBioscience), CD69 (conjugated to PerCp-Cy5.5, BD Biosciences), CD103 (conjugated to PE, eBioscience), FasL (conjugated to PE-Cy7, eBioscience), CD11c (conjugated to PE-TxR, Invitrogen), PD-1 (conjugated to PE-Cy7, BioLegend), annexin V (conjugated to PE, BD biosciences), and 7-AAD (BD Biosciences). Granzyme B (conjugated to PE, Life Technologies, Europe, Paisley, UK) and perforin (conjugated to APC, eBioscience) was stained intracellularly. The TCR repertoire was analyzed by using the mouse Vβ TCR screening panel (conjugated to FITC, BD Biosciences) staining Vβ 2, 3, 4, 5.1 + 5.2, 6, 7, 8.1 + 8.2, 8.3, 9, 10b, 11, 12, 13, 14, and 17a.

DC subsets were defined by using CD3 (conjugated to PE-Cy5, Tonbo Bioscience, San Diego, CA), CD19 (conjugated to PE-Cy5, eBioscience), CD11c (conjugated to PE-Cy7, eBioscience), MHCII (conjugated to APC-Cy7, BioLegend), CD11b (conjugated to BV605, BD Bioscience), CD24 (conjugated to eFl450, eBioscience), FcεRI (conjugated to biotin, eBioscience) combined with SAV (conjugated to CF594, BD bioscience), and a fixable live/dead marker in eFl506 (eBioscience).

Acquisition of 12-color samples was performed on a LSR II or Fortessa cytometer equipped with FACSDiva software (BD Biosciences). Final analysis and graphical output were performed using FlowJo software (Tree Star, Ashland, OR).

For soring of T cells, cells were stained as described and cell sorting was performed on a FACSAria II (BD Biosciences). The purity of sorted populations was $>95\%$.

Table 1 Q-PCR primer probe pairs

Target	Ensemble transcript	Fwd primer (5′→3′)	Rvs primer (5′→3′)	Probe #
CCR1	ENSMUST00000026911	GGACAAAATACTCTGGAAACACAGA	TGTGAAATCTGAAATCTCCATCC	73
CCR2	ENSMUST00000165984	TGTAAAGTAAGTGACAGTTTGCCTTT	GCTTGTTGCTATGTACAAACTGC	12
CCR3	ENSMUST00000039171	CATGCTCTAAGAATGAATATCTTTGGT	TGATTCCTGAGTAGCAGATAACCAT	55
CCR4	ENSMUST00000054414	TGTCCTCAGGATCACTTTCAGA	GGCATTCATCTTTGGAATCG	2
CCR5	ENSMUST00000111442	GAGACATCCGTTCCCCCTAC	GTCGGAACTGACCCTTGAAA	106
CCR7	ENSMUST00000103134	CAGGGAAACCCAGGAAAAAC	TCATCTTGGCAGAAGCACAC	77
CXCR1	ENSMUST00000053389	GGCATCTGGGGTCTATCTTTG	GTTTATATGCCTGGCGGAAG	13
CXCR2	ENSMUST00000106899	CCTGCTCTGTCACCGATG	CAGGGCAAAGAACAGGTCAG	62
CXCR3	ENSMUST00000056614	AAGCAGGGCAGCACGAGAC	GCATCTAGCACTTGACGTTCAC	3
Thpok	ENSMUST00000107435	CTTTGCCTGTGAGGTCTGC	CAGTGGGGGCACGAGTAG	2
Runx3	ENSMUST00000056977	GCCATCAAGGTCACTGTGG	AGGCCTTGGTCTGGTCTTCT	29
Hprt	ENSMUST00000026723	TCCTCCTCAGACCGCTTT	CCTGGTTCATCATCGCTAATC	95
L27	ENSMUST00000088784	TGAAAGGTTAGCGGAAGTGC	CATGAACTTGCCCATCTCG	3

Abbreviation: Q-PCR, quantitative PCR.

Cytokine staining: *in vitro* restimulation. Lung single-cell supsensions were restimulated with $NP_{ASNENMETM}$ peptide (10 μg ml^{-1}, AnaSpec, Seraing, Belgium) for 5 h at 37 °C in the presence of Golgi stop (BD Biosciences, 1/1,500) at a concentration of 5×10^6 cells per ml. After restimulation, cells were washed and stained extracellular, washed with PBS, and fixed with 2% paraformaldehyde, permeabilized with 0.5% saponin, and stained intracellularily for IFN-γ (Conjugated to PerCp-Cy5.5, eBioscience).

***In vivo* CD45 labeling**. Mice were injected i.v. with 3 μg of anti-CD45 antibody (AF700, eBioscience) and were killed 5 min later, blood was collected immediately before performing broncheoalveolar lavage. To remove blood from the capillary bed of the lungs, the lungs were flushed by injecting 20 ml PBS through the right ventricle. To protect the *in vivo* CD45 staining, lungs were dispersed mechanically instead of enzymatically by smashing them through an 40-μm filter before lysis of red blood cells.

BrdU incorporation assay. Mice were injected i.p. with 200 μl of 10 μg ml^{-1} BrdU (Sigma, Diegem, Belgium, 2 μg total per mouse) 6 d.p.i. and were killed 3.5 h after BrdU treatment. Lung cells were isolated as described above. Extracellular stained T cells were fixed and permeabilized by using the BrdU Flow Kit (BD Biosciences) according to the manufacturer's protocol in combination with an eFl450-labeled anti-BrdU antibody (eBiosciences).

Depletion of CD11c^{hi} cells. C57Bl/6 mice were irradiated sublethally (9 Gy) and reconstituted with 2×10^6 bone marrow cells i.v. from CD11c DTR transgenic donor mice 4 h after reconstitution. Mice were used for experiment at least 10 weeks after reconstitution. CD11c DTR chimeric mice were injected intraperitoneally with 200 ng diphteria toxin (DT) diluted in 200 μl PBS or with PBS 24 h before infection or 7 d.p.i. Lungs were analyzed 9 d.p.i.

Real-time quantitative reverse transcription PCR. Quantitative reverse transcription PCR for *Thpok*, *Runx3*, *Ccr1*, *Ccr2*, *Ccr3*, *Ccr4*, *Ccr5*, *Ccr7*, *Cxcr1*, *Cxcr2,* and *Cxcr3* were performed on cDNA samples obtained from sorted lung T-cell subsets. Total RNA was extracted using Tripure reagent (Sigma) according to the manufacturer's protocol. RNA was resuspended in Diethyl-polycarbonate (Sigma)-treated water. A total of 1 μg RNA was used for reverse transcription using the Transcriptor High Fidelity Reverse Transcriptase kit (Roche, Vilvoorde, Belgium) according to the manufacturer's protocol.

The subsequent target amplification on triplicates of each cDNA sample was performed using the Universal Probe Library system from Roche (that contains fluorescent hydrolysis probes of eight loked nucleic acids. Primers were designed with the help of the web-based application Probefinder (https://qpcr.probefinder.com) and a minimum of two primer pairs per target were analyzed. Primers were validated first using the LC480 SybrGreenI Master (Roche) with melting curve analysis (TM calling) in the LC480 Software and then using the LC480 Probes Master. Aspecific primer pairs were discarded. **Table 1** shows a comprehensive view of the primer/probe combinations chosen. PCR conditions were: 5′ pre-incubation at 95 °C followed by 45 amplification cycles of 10" at 95 °C, 10" at 60 °C, and 20" at 72 °C using a Lighcycler 480 (Roche). PCR amplifications for the housekeeping genes encoding *Hprt* or *L27* were performed during each run for each sample to allow normalization between samples.

Pulmonary DC-DNT co-cultures. Pulmonary DCs were sorted from the lungs of IAV-infected mice at 9 d.p.i. as lineage$^-$, alive, CD11c$^+$ MHCII$^+$ cells. DNT cells were sorted from lungs of infected mice at 9 d.p.i. as previously described and co-cultured with DCs in a 3.5:1 ratio in cell culture medium containing 10% fetal calf serum for 36 h.

Statistical analysis. All experiments were performed using four to six animals per group, unless mentioned otherwise. All experiments were performed at least two to three times. The difference between groups was calculated using the Mann–Whitney *U*-test for unpaired data (Prism version 6; GraphPad Software, La Jolla, CA). Data are depicted as mean ± s.e.m. Differences were considered significant when $P < 0.05$.

SUPPLEMENTARY MATERIAL is linked to the online version of the paper at http://www.nature.com/mi

ACKNOWLEDGMENTS

We thank the technical and logistic support of Dr Filipe Branco Madeira, Sofie De Prijck, Kim Deswarte, Manon Vanheerswynghels, Gert Van Isterdael, Justine Van Moorleghem, Karl Vergote, Dr Xavier Saelens, and Dr Michael Schotsaert for helpful discussions. K.N. is supported by a grant from FWO Flanders. B.N.L. is supported by Project grants of FWO Flanders, by an ERC Consolidator grant, and by a Ghent University MRP Grant (Group-ID consortium).

DISCLOSURE

The authors declared no conflict of interest.

REFERENCES

1. Brandes, M., Klauschen, F., Kuchen, S. & Germain, R.N. A systems analysis identifies a feedforward inflammatory circuit leading to lethal influenza infection. *Cell* **154**, 197–212 (2013).
2. Lambrecht, B.N. & Hammad, H. Lung dendritic cells in respiratory viral infection and asthma: from protection to immunopathology. *Ann. Rev. Immunol.* **30**, 243–270 (2012).
3. Galkina, E., Thatte, J., Dabak, V., Williams, M.B., Ley, K. & Braciale, T.J. Preferential migration of effector CD8+ T cells into the interstitium of the normal lung. *J. Clin. Invest.* **115**, 3473–3483 (2005).
4. Yoo, J.K., Fish, E.N. & Braciale, T.J. LAPCs promote follicular helperc T cell differentiation of Ag-primed CD4+ T cells during respiratory virus infection. *J. Exp. Med.* **209**, 1853–1867 (2012).
5. Hufford, M.M., Kim, T.S., Sun, J. & Braciale, T.J. Antiviral CD8+ T cell effector activities in situ are regulated by target cell type. *J. Exp. Med.* **208**, 167–180 (2011).
6. Topham, D.J., Tripp, R.A. & Doherty, P.C. CD8+ T cells clear influenza virus by perforin or Fas-dependent processes. *J. Immunol.* **159**, 5197–5200 (1997).
7. Johnson, S. *et al.* Selected Toll-like receptor ligands and viruses promote helper-independent cytotoxic T cell priming by upregulating CD40L on dendritic cells. *Immunity* **30**, 218–227 (2009).
8. Sun, J., Dodd, H., Moser, E.K., Sharma, R. & Braciale, T.J. CD4+ T cell help and innate-derived IL-27 induce Blimp-1-dependent IL-10 production by antiviral CTLs. *Nat. Immunol* **12**, 327–334 (2011).
9. Belz, G.T., Wodarz, D., Diaz, G., Nowak, M.A. & Doherty, P.C. Compromised influenza virus-specific CD8(+)-T-cell memory in CD4(+)-T-cell-deficient mice. *J. Virol* **76**, 12388–12393 (2002).
10. Lee, B.O. *et al.* CD4 T cell-independent antibody response promotes resolution of primary influenza infection and helps to prevent reinfection. *J. Immunol.* **175**, 5827–5838 (2005).
11. Brown, D.M., Lee, S., Garcia-Hernandez Mde, L. & Swain, S.L. Multifunctional CD4 cells expressing gamma interferon and perforin mediate protection against lethal influenza virus infection. *J. Virol.* **86**, 6792–6803 (2012).
12. Scherle, P.A., Palladino, G. & Gerhard, W. Mice can recover from pulmonary influenza virus infection in the absence of class I-restricted cytotoxic T cells. *J. Immunol.* **148**, 212–217 (1992).
13. Brown, D.M., Dilzer, A.M., Meents, D.L. & Swain, S.L. CD4 T cell-mediated protection from lethal influenza: perforin and antibody-mediated mechanisms give a one-two punch. *J. Immunol.* **177**, 2888–2898 (2006).
14. Joshi, N.S. *et al.* Inflammation directs memory precursor and short-lived effector CD8(+) T cell fates via the graded expression of T-bet transcription factor. *Immunity* **27**, 281–295 (2007).
15. Turner, D.L. *et al.* Lung niches for the generation and maintenance of tissue-resident memory T cells. *Mucosal Immunol.* **7**, 501–510 (2014).

16. Teijaro, J.R., Turner, D., Pham, Q., Wherry, E.J., Lefrancois, L. & Farber, D.L. Cutting edge: Tissue-retentive lung memory CD4 T cells mediate optimal protection to respiratory virus infection. *J. Immunol.* **187**, 5510–5514 (2011).
17. Hogan, R.J., Zhong, W., Usherwood, E.J., Cookenham, T., Roberts, A.D. & Woodland, D.L. Protection from respiratory virus infections can be mediated by antigen-specific CD4(+) T cells that persist in the lungs. *J. Exp. Med* **193**, 981–986 (2001).
18. Hogan, R.J. *et al.* Long-term maintenance of virus-specific effector memory CD8+ T cells in the lung airways depends on proliferation. *J. Immunol.* **169**, 4976–4981 (2002).
19. Liang, S., Mozdzanowska, K., Palladino, G. & Gerhard, W. Heterosubtypic immunity to influenza type A virus in mice. Effector mechanisms and their longevity. *J. Immunol* **152**, 1653–1661 (1994).
20. Wilkinson, P. *et al.* An open-ended plea for the development of a global database of HIV vaccine responses. *Curr. Opin. HIV AIDS* **7**, 10–16 (2012).
21. McKinstry, K.K. *et al.* Memory CD4+ T cells protect against influenza through multiple synergizing mechanisms. *J. Clin. Invest* **122**, 2847–2856 (2012).
22. Wu, T. *et al.* Lung-resident memory CD8 T cells (TRM) are indispensable for optimal cross-protection against pulmonary virus infection. *J. Leukoc. Biol* **95**, 215–224 (2014).
23. D'Acquisto, F. & Crompton, T. CD3+CD4-CD8- (double negative) T cells: saviours or villains of the immune response? *Biochem. Pharmacol.* **82**, 333–340 (2011).
24. Abraham, E., Freitas, A.A. & Coutinho, A.A. Purification and characterization of intraparenchymal lung lymphocytes. *J. Immunol.* **144**, 2117–2122 (1990).
25. Ibraghimov, A.R. & Lynch, R.G. T cell specialization at environmental interfaces: T cells from the lung and the female genital tract of lpr and gld mice differ from their splenic and lymph node counterparts. *Eur. J. Immunol.* **24**, 1848–1852 (1994).
26. Kawakami, K., Teruya, K., Tohyama, M., Kudeken, N., Yonamine, Y. & Saito, A. Mac1 discriminates unusual CD4-CD8- double-negative T cells bearing alpha beta antigen receptor from conventional ones with either CD4 or CD8 in murine lung. *Immunol. Lett* **46**, 143–152 (1995).
27. Takamoto, M., Kusama, Y., Takatsu, K., Nariuchi, H. & Sugane, K. Occurrence of interleukin-5 production by CD4- CD8- (double-negative) T cells in lungs of both normal and congenitally athymic nude mice infected with Toxocara canis. *Immunology* **85**, 285–291 (1995).
28. Watanabe, N. *et al.* Th1 and Th2 subsets equally undergo Fas-dependent and - independent activation-induced cell death. *Eur. J. Immunol* **27**, 1858–1864 (1997).
29. Oreshkova, T. *et al.* Beta(2) integrin deficiency yields unconventional double-negative T cells distinct from mature classical natural killer T cells in mice. *Immunology* **128**, 271–286 (2009).
30. Cowley, S.C., Meierovics, A.I., Frelinger, J.A., Iwakura, Y. & Elkins, K.L. Lung CD4-CD8- double-negative T cells are prominent producers of IL-17A and IFN-gamma during primary respiratory murine infection with Francisella tularensis live vaccine strain. *J. Immunol* **184**, 5791–5801 (2010).
31. Rajasekar, R. & Augustin, A. Selection of pulmonary CD4-, CD8-, alpha beta+ T cells expressing V beta 8T cell receptors. *Am. J. Respir. Cell Mol. Biol.* **10**, 79–84 (1994).
32. Augustin, A., Kubo, R.T. & Sim, G.K. Resident pulmonary lymphocytes expressing the gamma/delta T-cell receptor. *Nature* **340**, 239–241 (1989).
33. Godfrey, D.I., Stankovic, S. & Baxter, A.G. Raising the NKT cell family. *Nat. Immunol.* **11**, 197–206 (2010).
34. Godfrey, D.I., MacDonald, H.R., Kronenberg, M., Smyth, M.J. & Van Kaer, L. NKT cells: what's in a name?. *Nat. Rev. Immunol* **4**, 231–237 (2004).
35. Ford, M.S., Zhang, Z.X., Chen, W. & Zhang, L. Double-negative T regulatory cells can develop outside the thymus and do not mature from CD8+ T cell precursors. *J. Immunol* **177**, 2803–2809 (2006).
36. Kadena, T. *et al.* TCR alpha beta+ CD4- CD8-T cells differentiate extrathymically in an lck-independent manner and participate in early response against Listeria monocytogenes infection through interferon-gamma production. *Immunology* **91**, 511–519 (1997).
37. Mohamood, A.S. *et al.* Fas-mediated apoptosis regulates the composition of peripheral alphabeta T cell repertoire by constitutively purging out double negative T cells. *PLoS One* **3**, e3465 (2008).
38. Mehal, W.Z. & Crispe, I.N. TCR ligation on CD8+ T cells creates double-negative cells *in vivo*. *J. Immunol.* **161**, 1686–1693 (1998).
39. Naito, T., Tanaka, H., Naoe, Y. & Taniuchi, I. Transcriptional control of T-cell development. *Int. Immunol* **23**, 661–668 (2011).
40. Kedzierska, K., Turner, S.J. & Doherty, P.C. Conserved T cell receptor usage in primary and recall responses to an immunodominant influenza virus nucleoprotein epitope. *Proc. Natl Acad. Sci. USA* **101**, 4942–4947 (2004).
41. Lantz, O. & Bendelac, A. An invariant T cell receptor alpha chain is used by a unique subset of major histocompatibility complex class I-specific CD4+ and CD4-8- T cells in mice and humans. *J. Exp. Med* **180**, 1097–1106 (1994).
42. Kawano, T. *et al.* CD1d-restricted and TCR-mediated activation of valpha14 NKT cells by glycosylceramides. *Science* **278**, 1626–1629 (1997).
43. Wherry, E.J. *et al.* Lineage relationship and protective immunity of memory CD8 T cell subsets. *Nat. Immunol* **4**, 225–234 (2003).
44. Mueller, S.N., Gebhardt, T., Carbone, F.R. & Heath, W.R. Memory T cell subsets, migration patterns, and tissue residence. *Annu. Rev. Immunol* **31**, 137–161 (2013).
45. Grebe, K.M., Yewdell, J.W. & Bennink, J.R. Heterosubtypic immunity to influenza A virus: where do we stand? *Microbes Infect* **10**, 1024–1029 (2008).
46. Kreijtz, J.H. *et al.* Primary influenza A virus infection induces cross-protective immunity against a lethal infection with a heterosubtypic virus strain in mice. *Vaccine* **25**, 612–620 (2007).
47. Plantinga, M. *et al.* Conventional and monocyte-derived CD11b+ dendritic cells initiate and maintain T helper 2 cell-mediated immunity to house dust mite allergen. *Immunity* **38**, 322–335 (2013).
48. GeurtsvanKessel, C.H. *et al.* Clearance of influenza virus from the lung depends on migratory langerin+CD11b- but not plasmacytoid dendritic cells. *J. Exp. Med* **205**, 1621–1634 (2008).
49. Kim, T.S., Gorski, S.A., Hahn, S., Murphy, K.M. & Braciale, T.J. Distinct dendritic cell subsets dictate the fate decision between effector and memory CD8(+) T cell differentiation by a CD24-dependent mechanism. *Immunity* **40**, 400–413 (2014).
50. Kim, T.S., Hufford, M.M., Sun, J., Fu, Y.X. & Braciale, T.J. Antigen persistence and the control of local T cell memory by migrant respiratory dendritic cells after acute virus infection. *J. Exp. Med.* **207**, 1161–1172 (2010).
51. Gao, J.F. *et al.* Regulation of antigen-expressing dendritic cells by double negative regulatory T cells. *Eur. J. Immunol* **41**, 2699–2708 (2011).
52. Chang, J.C., Zhang, L., Distler, S.G., Ziang, G. & Kaplan, A.M. Characterization and function of CD3+ CD4- CD8- TcR-alpha beta bearing cells infiltrating the lung during the immune response. *Reg. Immunol.* **4**, 25–33 (1992).
53. Rossjohn, J., Pellicci, D.G., Patel, O., Gapin, L. & Godfrey, D.I. Recognition of CD1d-restricted antigens by natural killer T cells. *Nat. Rev. Immunol.* **12**, 845–857 (2012).
54. Liao, C.M., Zimmer, M.I. & Wang, C.R. The functions of type I and type II natural killer T cells in inflammatory bowel diseases. *Inflamm. Bowel Dis.* **19**, 1330–1338 (2013).
55. Priatel, J.J., Utting, O. & Teh, H.S. TCR/self-antigen interactions drive double-negative T cell peripheral expansion and differentiation into suppressor cells. *J. Immunol* **167**, 6188–6194 (2001).
56. Hayes, S.M., Li, L. & Love, P.E. TCR signal strength influences alphabeta/gammadelta lineage fate. *Immunity* **22**, 583–593 (2005).
57. Paget, C. & Trottein, F. Role of type 1 natural killer T cells in pulmonary immunity. *Mucosal Immunol* **6**, 1054–1067 (2013).
58. Edholm, E.S., Grayfer, L. & Robert, J. Evolution of nonclassical MHC-dependent invariant T cells. *Cell. Mol. Life Sci.* **71**, 4763–4780 (2014).
59. Le Bourhis, L., Guerri, L., Dusseaux, M., Martin, E., Soudais, C. & Lantz, O. Mucosal-associated invariant T cells: unconventional development and function. *Trends Immunol* **32**, 212–218 (2011).
60. Hedrich, C.M. *et al.* cAMP-responsive element modulator alpha (CREMalpha) trans-represses the transmembrane glycoprotein CD8 and contributes to the generation of CD3+CD4-CD8- T cells in health and disease. *J. Biol. Chem.* **288**, 31880–31887 (2013).

61. Hedrich, C.M. *et al.* cAMP responsive element modulator (CREM) alpha mediates chromatin remodeling of CD8 during the generation of CD3 + CD4- CD8- T cells. *J. Biol. Chem* **289**, 2361–2370 (2014).
62. Anderson, K.G. *et al.* Cutting edge: intravascular staining redefines lung CD8 T cell responses. *J. Immunol* **189**, 2702–2706 (2012).
63. Antonelli, L.R. *et al.* Disparate immunoregulatory potentials for double-negative (CD4- CD8-) alpha beta and gamma delta T cells from human patients with cutaneous leishmaniasis. *Infect. Immun.* **74**, 6317–6323 (2006).
64. Pinheiro, M.B. *et al.* CD4-CD8-alphabeta and gammadelta T cells display inflammatory and regulatory potentials during human tuberculosis. *PLoS One* **7**, e50923 (2012).
65. Martin, E. *et al.* Stepwise development of MAIT cells in mouse and human. *PLoS Biol.* **7**, e54 (2009).
66. Le Bourhis, L. *et al.* Antimicrobial activity of mucosal-associated invariant T cells. *Nat. Immunol* **11**, 701–708 (2010).
67. Ross, T.L. *et al.* Role of CD4 + , CD8 + and double negative T-cells in the protection of SCID/beige mice against respiratory challenge with Rhodococcus equi. *Can. J. Vet. Res.* **60**, 186–192 (1996).
68. Zhang, Z.X., Yang, L., Young, K.J., DuTemple, B. & Zhang, L. Identification of a previously unknown antigen-specific regulatory T cell and its mechanism of suppression. *Nat. Med* **6**, 782–789 (2000).
69. Hillhouse, E.E. & Lesage, S. A comprehensive review of the phenotype and function of antigen-specific immunoregulatory double negative T cells. *J. Autoimmun.* **40**, 58–65 (2013).
70. Liang, Q. *et al.* Double Negative (DN) [CD3(+)CD4(-)CD8(-)] T cells correlate with disease progression during HIV infection. *Immunol. Invest* **42**, 431–437 (2013).
71. Miao, J. *et al.* Percentages of CD4 + CD161 + and CD4-CD8-CD161 + T Cells in the synovial fluid are correlated with disease activity in rheumatoid arthritis. *Mediators Inflamm.* **2015**, 563713 (2015).
72. Alunno, A. *et al.* IL-17-producing CD4-CD8- T cells are expanded in the peripheral blood, infiltrate salivary glands and are resistant to corticosteroids in patients with primary Sjogren's syndrome. *Ann. Rheum. Dis* **72**, 286–292 (2013).
73. Alunno, A. *et al.* CD4(-)CD8(-) T-cells in primary Sjogren's syndrome: association with the extent of glandular involvement. *J. Autoimmun.* **51**, 38–43 (2014).